Since January 2020 Elsevier has created a COVID-19 resource centre with free information in English and Mandarin on the novel coronavirus COVID-19. The COVID-19 resource centre is hosted on Elsevier Connect, the company's public news and information website.

Virus Research 202 (2015) 3–11

Contents lists available at ScienceDirect

Virus Research

journal homepage: www.elsevier.com/locate/virusres

Looking for a needle in a haystack: Cellular proteins that may interact with the tyrosine-based sorting signal of the TGEV S protein

Anna Trincone [1], Christel Schwegmann-Weßels *

Institute for Virology, Department of Infectious Diseases, University of Veterinary Medicine Hannover, Bünteweg 17, 30559 Hannover, Germany

ARTICLE INFO

Article history:
Available online 4 December 2014

Keywords:
Coronavirus
TGEV
Spike protein
Assembly
Filamin A
Cellular interaction candidates

ABSTRACT

The spike protein S of transmissible gastroenteritis virus, an *Alphacoronavirus*, contains a tyrosine-based sorting signal that is responsible for ERGIC retention and may be important for a correct viral assembly process. To find out whether the S protein interacts with cellular proteins via this sorting signal, a pulldown assay with GST fusion proteins was performed. Filamin A has been identified as a putative interaction candidate. Immunofluorescence assays confirmed a co-localization between the TGEV S protein and filamin A. Further experiments have to be performed to prove a significant impact of filamin A on TGEV infection. Different approaches of several researchers for the identification of cellular interaction candidates relevant for coronavirus replication are summarized. These results may help in the future to identify the role of cellular proteins during coronavirus assembly at the ER-Golgi intermediate compartment.

1. Introduction

Coronaviruses assemble intracellularly and acquire their envelope through a budding process at the ER-Golgi intermediate compartment (ERGIC) (Bost et al., 2001; Krijnse-Locker et al., 1994; Tooze et al., 1984). Coronavirus particles consist of a positive-stranded RNA genome and a canonical set of M, E, S, and N proteins; and in some cases an HE protein. Several researchers have addressed the localization of the viral structural proteins M, E, S, and N and their interactions (with each other and/or cellular proteins).

The coronavirus M protein appears to be the key player of coronavirus particle assembly. It was shown to interact with each of the other structural proteins: E, HE, N, and S (de Haan et al., 1999; Escors et al., 2001; He et al., 2004; Nguyen and Hogue, 1997). Expression of M and E protein is sufficient to assemble enveloped virus-like particles. The S protein is incorporated into these particles if present (Godeke et al., 2000; Vennema et al., 1996). The coronavirus M protein is localized in the *cis*- or *trans*-Golgi as reported for TGEV, IBV, and MHV (Klumperman et al., 1994; Locker et al., 1994; Machamer et al., 1990). The interaction of the IBV M and E proteins are mediated by their cytoplasmic domains (Corse and Machamer, 2003; Lim and Liu, 2001). It was shown that the E proteins of IBV and SARS-CoV contain a Golgi-targeting signal (Cohen et al., 2011; Corse and Machamer, 2000, 2002).

The S proteins of TGEV and IBV are retained at the ERGIC whereas the SARS-CoV S protein is transported to the cell surface in single expression experiments (Paul et al., 2014; Schwegmann-Wessels et al., 2004; Simmons et al., 2004; Winter et al., 2008). The SARS-CoV S protein is retained intracellularly through its interaction with the M protein (McBride et al., 2007; McBride and Machamer, 2010).

The coronavirus N protein is localized to the cytoplasm. Additionally, some smaller parts of the N protein were shown to be localized in the nucleolus (Hiscox et al., 2001; Wurm et al., 2001). After infection, the N protein of TGEV is predominantly localized in ERGIC-enriched fractions (Calvo et al., 2005). For the SARS-CoV N protein, several groups have found that it is localized, in single expression as well as in infection, in the cytoplasm and not in the nucleolus (Rowland et al., 2005; Timani et al., 2005; You et al., 2005).

An overview over the approaches to analyze the interaction of structural viral proteins like the N or the S protein with cellular proteins and the influence of cellular proteins on coronavirus assembly is presented in the following sections.

2. Analysis of coronavirions by mass spectrometry for the presence of viral and cellular proteins

Little is known about the involvement of cellular proteins during the viral assembly process. Different approaches have been applied

* Corresponding author at: Institute for Virology, Department of Infectious Diseases, University of Veterinary Medicine Hannover, Foundation, Bünteweg 17, 30559 Hannover, Germany Tel.: +49 511 9538842; fax: +49 511 9538898.
E-mail address: christel.schwegmann@tiho-hannover.de (C. Schwegmann-Weßels).
[1] Present address: Centre for Pharmacology and Toxicology, Institute for Pharmaco- and Toxicogenomics, Feodor-Lynen-Str. 35, 30625 Hannover, Germany.

http://dx.doi.org/10.1016/j.virusres.2014.11.029
0168-1702/

in recent years to identify cellular host factors involved in virus assembly. Mass spectrometry analysis of purified virions revealed that a variety of host cellular proteins are included in purified viral particles as well as non-structural viral proteins like nsp2, 3, and 5 for the severe acute respiratory syndrome coronavirus (SARS-CoV) and RNA-dependent RNA polymerase, nsp 2, 3, and 8 for the transmissible gastroenteritis coronavirus (TGEV) (Neuman et al., 2008; Nogales et al., 2012).

Neuman et al. (2008) collected SARS-CoV grown on Vero-E6 cells by polyethylene glycol precipitation and purified the virus particles by banding on a sucrose density gradient. These purified samples were compared to samples treated with DNase I and proteinase K after the sucrose gradient purification step. A two-dimensional liquid chromatography MS/MS analysis was performed after in-solution digestion of the proteins. Two different extraction techniques were used: TCA precipitation and methanol delipidation, as not all proteins could be detected with either extraction procedure. In addition to the aforementioned viral proteins, Neuman et al. (2008) identified nearly 200 host proteins present in purified SARS-CoV related to different cellular functions. Three COPI coatomer components (α-COB, β-COP, and γ-COP) and ADP-ribosylation factor 4 (ARF4), a protein involved in COPI trafficking, were detected in purified SARS-CoV particles by Neuman and coworkers. The COPI coatomer is involved in the retrograde vesicular transport between the ER and the Golgi, in transport between Golgi stacks, and in transport from the intermediate compartment to the *cis*-Golgi (Kirchhausen, 2000; Volpicelli-Daley et al., 2005). ARF4 and COPI proteins are known to be abundant at membranes of the ERGIC, the site of coronavirus budding (Krijnse-Locker et al., 1994; Volpicelli-Daley et al., 2005). Mc Bride et al. demonstrated binding of COPI by a dibasic motif in the cytoplasmic tail of the SARS-CoV spike protein (McBride et al., 2007). Probably, COP and ARF proteins are involved in virus assembly and budding. Further host factors present in the ERGIC may also play a role, although they were not detected by the approach of Neuman and coworkers. Integral membrane proteins and membrane-associated proteins were underrepresented in the results of their study. The reason for this low amount of detected membrane proteins may be technical limitations, the biochemical properties of the proteins like low solubility or limited protease accessibility, or/and the exclusion of host proteins from the viral membranes by the M protein networks (de Haan et al., 2000).

In a proteomic analysis of an avian coronavirus, in purified infectious bronchitis virus (IBV) particles Kong and coworkers detected about 60 host proteins in addition to the viral proteins S and N (Kong et al., 2010). Kong et al. used IBV strain H52 grown on 10-day-old SPF embryonated chicken eggs. After concentration through a 20% sucrose cushion, virus particles were purified through a discontinous sucrose gradient. Like Neuman and coworkers, Kong et al. confirmed the purity of their preparation by electron microscopy analysis. For their protein composition analysis, Kong et al. extracted the proteins from purified IB virions for two-dimensional gel electrophoresis (2-DE) profiles. All detected protein spots were excised from the gel and in-gel digested with trypsin. A MALDI-TOF/TOF analysis revealed the presence of the two viral proteins N and S and about 60 host proteins. Among them, 21 host proteins detected in purified IBV particles have not been described to be present in other virions (Kong et al., 2010). The reason for this may be that the virus was grown on embryonated eggs rather than in cultured cells, and that the amniotic fluid was used for virion purification. In contrast to Neuman et al., Kong and coworkers did not find ARF or COP proteins in their preparations. This may be due to the use of amniotic fluid for virion purification. Another group of host proteins, the heat-shock proteins (HSPs) were found by both groups (Kong et al., 2010; Neuman et al., 2008). HSPs are multifunctional proteins that facilitate protein folding and unfolding, prevent protein aggregation, are involved in cell signaling, and participate in vesicular transport processes. Therefore, these proteins may play a role for coronavirus assembly. Whereas Kong et al. have found HSP70 and HSP90 incorporated into IBV, Neuman et al. specifically identified HSP90 and classified HSP70 as a background protein. Furthermore, Kong et al. detected several cytoskeletal proteins that were incorporated into or associated with IB virions. Actins and tubulins as main cytoskeletal proteins may actively participate in moving viral components to the assembly sites. An interaction of the IBV M protein with β-actin and its putative role in virus assembly has been reported (Wang et al., 2009). Neuman et al. also detected cytoskeletal proteins in their SARS-CoV preparations. In addition to actin and tubulin, they identified myosin, filamin, and fibronectin. All these cytoskeletal proteins were also found in their background control samples but as they were consistently detected in proteinase K treated samples as well, they may have been incorporated into virions.

After purification of TGEV particles (sedimentation through a 31% sucrose cushion, purification over a continuous sucrose density gradient), Nogales and coworkers performed an SDS-PAGE, excised the proteins from the gel, and analyzed them by MALDI-TOF after trypsin digestion (Nogales et al., 2012). In addition to viral proteins, they detected a large number of cellular proteins identical to those detected in the above described SARS-CoV and IBV proteomics. As reported for SARS-CoV and IBV particles, HSP90 and the cytoskeletal proteins β-actin and tubulin were identified by Nogales et al. in purified TGEV. Cytoskeletal proteins interact with numerous viral proteins. The transport machinery of actins can be involved at every step of the infectious cycle. For several viruses the presence of actin, tubulin, or other cytoskeletal proteins in virion preparations has been reported (Cantin et al., 2005; Chertova et al., 2006; Shaw et al., 2008). Nevertheless, some cellular proteins identified by the analysis of coronavirions by mass spectrometry simply may have been incorporated into the virions because of their high abundance at the viral budding site. In addition, some proteins may just adhere at the virion surface without being removed by proteinase K treatment. On the other hand, it is possible that some detected cellular proteins may have so far unknown functions different from those for which they are known.

3. Quantitative analysis of the cellular proteome after coronavirus infection

To identify which cellular proteins are up- or down-regulated due to a TGEV infection, Zhang et al. (2013) used the method of two-dimensional difference gel electrophoresis (2-DIGE) coupled with an analysis of the spots by MALDI-TOF-TOF/MS. For this purpose, swine testicular (ST) cells were compared at 48 h p.i. to mock-infected ST cells using CyDyes for staining of the different samples. For TGEV-infected ST cells, 33 differentially expressed protein spots were found, 23 of them up-regulated and 10 down-regulated during infection. Cytoskeletal proteins like β-actin as microfilament-associated protein, α- and β-tubulin as microtubule-associated proteins, and vimentin as intermediate filament protein have been identified to be differentially expressed in ST cells after TGEV infection. Actin and tubulin as components of the cytoskeleton play important roles in the life cycle of many viruses (Cudmore et al., 1997; Greber and Way, 2006; Ploubidou and Way, 2001; Radtke et al., 2006). The upregulation of β-actin and tubulins in TGEV-infected ST cells may be due to intracellular transport of viral proteins from the ER to the intermediate compartment and the Golgi apparatus with help of the cytoskeleton. Additionally, annexin 8 and annexin 4 were differentially expressed in TGEV-infected ST cells. Both are known as proteins involved in vesicular transport (Zhang et al., 2013).

Cao and co-workers used the same approach to analyze the differentially expressed proteins after an IBV infection (Cao et al., 2011, 2012). They analyzed chicken embryonic trachea and kidney tissues after *in ovo* infection by IBV using 2-DE with Coomassie Blue staining and MALDI-TOF-TOF/MS. Here, they found 17 differentially expressed proteins from tracheal tissue and 19 from kidney tissue (Cao et al., 2011). In their subsequent report, they analyzed the differentially expressed proteins in trachea and kidney tissues from chicken at different stages infected in vivo with two different IBV strains – a highly virulent and an attenuated one (Cao et al., 2012). In addition to their methods in the previous work, they applied 2-DIGE which is known to be much more sensitive than 2-DE. Here they reported that 58 differentially expressed proteins were detected. Some of the detected proteins showed differences in their expression level after infection with the virulent strain compared to the attenuated one. The changes occurred mainly in proteins with functions in cytoskeleton organization, anti-oxidative stress, and stress response. Like Zhang et al., Cao and co-workers identified different annexins (annexin A2 and annexin A5) being differentially expressed upon IBV infection. Annexins are calcium-dependent phospholipid-binding proteins that are able to associate with the cytoskeleton (Moss and Morgan, 2004). Some annexins are known to have strong vesicle-aggregating activity (Donnelly and Moss, 1997). Annexin A2 was identified as an important host factor in the life cycle of several viruses being involved in virus assembly, release or replication (Backes et al., 2010; Beaton et al., 2002; Harrist et al., 2009; Ryzhova et al., 2006). The expression of Annexin A2 and A5 has also been found to be altered after IBV infection of Vero and avian cells (Emmott et al., 2010a,b).

Emmott and co-workers used a different quantitative proteomic approach, based on stable isotope labeling with amino acids in cell culture (SILAC), to analyze changes in the cytoplasmic, nuclear, and nucleolar proteomes from Vero cells after infection with IBV Beaudette (Emmott et al., 2010a). The cells were fractionated after isotope labeling into cytoplasmic, nuclear, and nucleolar extracts to reduce sample complexity but also to find out the different trafficking pathways of proteins. After separation by SDS-PAGE and Coomassie staining, each protein band was cut out from the gel and in gel-digested with trypsin. The proteins were then identified and quantified by LC–MS/MS. After IBV infection of Vero cells, one protein was reduced and 66 proteins were enriched in the cytoplasmic fraction ($\geq$2.0-fold). In the nuclear fraction, 35 proteins were reduced and 5 proteins were enriched. In the nucleolar proteome, 12 proteins were reduced and 22 proteins showed an increase. The results were analyzed using bioinformatic tools and classified according to their function. A network pathway analysis ruled out that proteins involved in cellular assembly, organization, morphology, signaling, and growth were differentially expressed in Vero cells due to IBV infection. Many of these proteins were e.g. linked to the NF-κB and AP-1 signaling cascades.

The two proteins myosin VI (MYO6) that is involved in vesicular trafficking (Aschenbrenner et al., 2003), and vimentin, a major part of type III intermediate filaments of the cytoskeleton, were both enriched after IBV infection. MYO6 was 90-fold more abundant in the nuclear proteome than in mock-infected cells and showed a different distribution in mock-infected and IBV-infected cells. In mock-infected cells this protein was distributed predominantly in the cytoplasm whereas, it showed perinuclear and nuclear punctate staining in IBV-infected cells. Vimentin lost its enrichment in the perinuclear region due to syncytia formation of IBV-infected cells. Among the viral proteins, Emmott and coworkers detected the M and the N protein. The M protein was present in the cytoplasmic proteome whereas the N protein was detectable in all three fractions. In an additional paper, Emmott et al. (2010b) reported the analysis of the avian nucleolar proteome by using a chicken fibroblast cell line (DF-1 cells). Again, they compared mock-infected cells with IBV-infected cells using SILAC.

Jiang et al. (2005) used a technique similar to SILAC, the isotope-coded affinity tag technology (ICAT) coupled with two-dimensional LC–MS/MS, to quantify the changes in SARS-CoV infected Vero E6 cells compared to uninfected cells. Additionally, Jiang and coworkers applied 2-DIGE followed by ESI-MS/MS identification. In the 2-DIGE approach, 63 proteins were identified with 17 of them down-regulated and 13 proteins that were up-regulated. By using the ICAT method, Jiang et al. identified 119 proteins that were up-regulated and 48 proteins, that were down-regulated by SARS-CoV infection. Jiang et al. compared the two methods they used to identify alteration in the cellular proteome after infection with SARS-CoV. Although only 15 differential proteins were identified with both methods, the overall expression alterations were similar using 2-DIGE and ICAT. The up-regulated proteins found in the infected cells were mainly present in the nuclei, whereas the down-regulated proteins distributed within the cell. The two methods, 2-DIGE and ICAT, were found by Jiang et al. to be complementary to each other. Proteins with high molecular mass or with low abundance were detected by ICAT whereas proteins in a certain low molecular mass range and cysteine-free proteins were detected by 2-DIGE. Among other proteins, Jiang et al. demonstrated the up-regulation of α-tubulin and HSP90 after SARS-CoV infection of Vero E6 cells. These two proteins were also found by Neuman and coworkers in SARS-CoV purified particles (Neuman et al., 2008).

Vogels et al. (2011) performed SILAC to identify host factors involved in mouse hepatitis virus (MHV) replication. Vogels and coworkers focused on the secretory pathway and investigated the changes in protein composition of an isolated Golgi-enriched fraction after infection of HeLa cells stably expressing the MHV receptor CEACAM1a. The cells were infected with MHV A59 (MOI of 50) and used 6 h p.i. for the isolation of the Golgi-enriched fraction. Proteins from this fraction were separated by SDS-PAGE, in-gel digested with trypsin, and applied to LC–MS/MS. Due to the stable isotope labeling, Vogels et al. could identify 43 proteins which were enriched and 73 which were depleted after MHV infection in the Golgi-enriched fraction. From these affected proteins, 13 proteins were selected and analyzed for their functional relevance in MHV replication by transfecting cells with siRNA. Three of them were further studied by overexpression of GFP-fusion constructs. With these experiments, Vogels et al. showed that C11orf59, GLG1, and SEC22B may play a role in MHV replication. Depletion of SEC22B, a vesicle-trafficking protein, led to an increase in infectious progeny virus. SEC22B is involved in vesicular trafficking between ER and Golgi (Hay et al., 1998). SEC22B might somehow interfere with MHV at the coronavirus assembly and budding site.

In contrast to other reports, Vogels and coworkers focussed on the secretory pathway and analyzed the cells at 6 h p.i. The aforementioned studies have been performed after 24–48 h p.i. to get a high yield of viral replication, virus-infected cells, and/or viral particles in the cell culture supernatant. To identify host proteins involved in virus assembly, proteomics at a time point relevant for virus assembly may help to catch important cellular proteins. Therefore, the approach by Vogels et al. may give interesting insights into this step of viral replication. In addition to the further described proteins C11orf59, GLG1, and SEC22B, Annexin A2 was enriched in Golgi fractions after MHV infection of the cells. This protein was also shown to be involved in IBV infection (Cao et al., 2011, 2012). Annexin A2 may play a role in coronavirus assembly. For other viruses like Hepatitis C virus and HIV, annexin A2 was found to be involved in virus assembly (Backes et al., 2010; Harrist et al., 2009).

Approaches like the SILAC method in which not only interaction partners are identified, but also an enrichment or depletion of

proteins due to virus infection can be measured will help to further analyze the role of cellular proteins in virus assembly and budding.

Despite the differerences in cellular proteins found by several researchers after infection with coronaviruses like TGEV, IBV, SARS-CoV, and MHV, there are some repetitive proteins that might be involved in the steps of coronavirus assembly and viral protein trafficking. Especially cytoskeletal proteins like actin and tubulin, HSP90, vimentin, and annexins have been reported by different groups using different experimental approaches.

4. Identification of cellular candidates interacting with coronaviral proteins

Stable isotope labeling with amino acids in cell culture (SILAC) is not only suitable for the comparison of infected with uninfected cells, but can also be used to identify potential interactomes of specific viral proteins. To find out which cellular proteins are able to bind to the IBV N protein, Emmott et al. used SILAC and coupled it with a GFP-pulldown method followed by LC-MS/MS (Emmott et al., 2013). For this purpose, the two GFP-fusion proteins, EGFP-N (encoding for the IBV N protein) and EGFP, were expressed in 293 T cells. After isotope labeling and cell lysis, the GFP-fusion proteins were immunoprecipitated using GFP-trap beads. Protein samples recovered from the GFP-trap were separated by SDS-PAGE and gel slices were in-gel digested with trypsin. Resulting peptides were identified and quantified by LC–MS/MS. In total, 142 cellular proteins appeared to interact specifically with the IBV N protein. Over a third of the identified proteins were ribosomal proteins. Three proteins, involved in the formation of cytoplasmic stress granules, have also been identified: Caprin-1, G3BP-1, and G3BP-2. Furthermore, Emmott and coworkers analyzed the co-localization of selected cellular proteins with the IBV N protein in IBV-infected cells. To show the relevance of the proteins in IBV infection, siRNA experiments were performed. Emmott et al. concluded in this paper that the N protein presumably did not interact with all 142 proteins individually; moreover, they found many complexes of cellular proteins, which could bind to the N protein via different hub proteins, such as nucleolin.

The yeast-two-hybrid analysis is another approach to identify protein–protein interactions. Von Brunn and collegues used this method to analyze the intraviral protein–protein interactions as well as the virus-host interactions related to SARS-CoV-derived proteins (Pfefferle et al., 2011; von Brunn et al., 2007). With a high-throughput yeast two hybrid screen (HTY2H), Pfefferle and coworkers found 942 gene hits in their interaction screening of the SARS-CoV ORFeome and a cDNA library derived from human brain as well as an additional library containing ORFs encoding 5000 human proteins (Pfefferle et al., 2011). These hits were divided into four confidence categories with 132 hits in category A (highly confident interaction partners found more than once in one screen or several screens) and 383 hits in category B (single hits). The cDNAs of 86 interaction candidates were cloned in a luciferase vector, and interaction with the SARS-CoV ORFs, cloned in-frame with protein A domains, was validated by immunoprecipitation of the SARS-CoV proteins and subsequent measurement of the luciferase activity. About 48% of category A and 36% of category B interaction candidates were successfully validated with this approach. Pfefferle et al. compared their results with data derived from published literature and searched for preferentially targeted protein complex subunits. The four following complexes were found to be specifically enriched: respiratory chain complex I, cytoplasmic ribosome, 60S ribosomal subunit, and the LCR-associated remodeling complex.

The nonstructural protein Nsp1 from SARS-CoV showed a particularly interesting candidate interaction network. Therefore, Pfefferle et al. (2011) concentrated on this viral protein and identified immunophilins as interaction partners of Nsp 1. The Calcineurin/NFAT pathway is modulated by immunophilins being involved in immune cell activation and induction of interleukin 2. With their approach, Pfefferle and coworkers could identify cyclosporine A as a pan-coronavirus inhibitor that interacts with cyclophilins and leads to a block in coronavirus replication.

A yeast two-hybrid screen was also used by Zhou et al. (2008) to find interaction candidates for the SARS-CoV N protein. The researchers detected a protein–protein association between the translation elongation factor 1 α (EF1α) and the SARS-CoV N protein. They demonstrated direct binding between these two proteins by using GST-fusion proteins. Furthermore, Zhou and coworkers demonstrated that the SARS-CoV N protein inhibited protein translation and cytokinesis by aggregating EF1α.

Wang et al. (2009) applied the yeast two-hybrid screen approach (Y2H) to detect the interaction of the IBV M protein with β-actin. They used IBV nonstructural and structural proteins as bait. In a screen with a human cDNA library, they found that the C-terminal cytoplasmic portion of the IBV M protein was able to interact with β-actin. Further co-localization and co-immunoprecipitation experiments confirmed this result obtained by Y2H. The region on the M protein responsible for the interaction with β-actin was mapped by constructing deletion mutants and one double mutant and analyzing them for their interaction with actin in yeast cells. Wang and coworkers concluded that the amino acids A159 and K160 are important for the interaction of the IBV M protein with β-actin. Furthermore, they postulated that actin filaments may be involved in assembly and budding of IB virions. As the M protein is the key player of viral assembly, its interaction with elements of the cytoskeleton may help to complete the IBV replication cycle. Free energy, gained by the interaction of the M protein with host proteins, may be necessary to complete coronavirus envelope assembly. Actin polymerization can serve as additional force for membrane bending during budding (Gov and Gopinathan, 2006). Additionally, actin may be involved in the movement of viral proteins to the coronavirus assembly site. Actin was found to be incorporated into IB virions as well as into other coronavirus particles (Kong et al., 2010; Neuman et al., 2008; Nogales et al., 2012). Actin-binding proteins like tropomyosin were found to be enriched after IBV infection (Cao et al., 2011, 2012).

5. The GST pull-down method to identify cellular interaction partners of coronavirus proteins

Glutathione-S-transferase (GST)-fusion proteins have been used for more than 20 years for the synthesis of recombinant proteins in bacterial expression systems (Smith and Johnson, 1988). The GST pull-down method can be used to identify interactions between one known and several unkown proteins or to demonstrate and analyze an already identified protein interaction (Kaelin et al., 1991; Orlinick and Chao, 1996; Sambrook and Russell, 2006).

Based on the results reported by Zhou et al. (2008), Zhang et al. (2014) recently analyzed the interaction of EF1α with the nucleocapsid protein of transmissible gastroenteritis coronavirus (TGEV). Using a GST pull-down assay after expressing the GST-N fusion protein in *Escherichia coli* BL21, Zhang et al. confirmed the interaction between TGEV N and EF1α. In TGEV-infected ST cells, the viral N protein co-localized with EF1α. A knockdown of EF1α protein in ST cells using siRNA led to a reduction in viral N protein expression as well as in TGEV replication.

Using a similar GST pull-down approach, McBride and coworkers demonstrated that a dibasic motif present in the C-terminal part of the SARS-CoV S and IBV S protein cytoplasmic domain interacts with COPI (McBride et al., 2007). For this purpose, the C-terminal

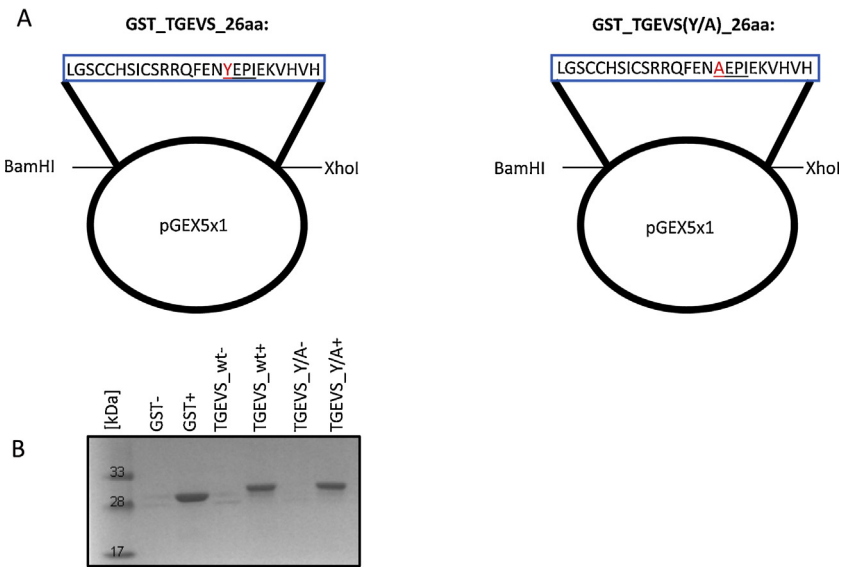

Fig. 1. GST fusion proteins used throughout the study. (A) The part of the TGEV S gene encoding for the C-terminal 26 amino acids was cloned in the vector pGEX5x1. The sequence of the two GST fusion proteins, GST_TGEVS_26aa (short: TGEVS_wt) and GST_TGEVS(Y/A)_26aa (short: TGEVS_Y/A), is shown in blue boxes with the amino acid differences highlighted in red. The tyrosine-based sorting signal is underlined. (B) The bacterial cell lysates were purified with Glutathione Agarose 4B and the GST fusion proteins were detected after SDS-PAGE with Coomassie Blue staining at a molecular mass of about 30 kDa. All three proteins – GST, TGEVS_wt, and TGEVS_Y/A – showed a positive signal after IPTG induction of bacteria (+).

29 amino acids from the coronavirus S protein were fused to GST by using the expression vector pGEX2T. The respective constructs were transformed into competent *E. coli* BL21 cells and GST fusion proteins were purified from bacterial cell lysates using Glutathione-Sepharose 4B beads. To demonstrate binding to COPI, McBride et al. incubated 10 μg of each purified GST fusion protein with CHO cell lysates on Glutathione-Sepharose 4B beads. In a following Western blot analysis they detected COPI in the GST-IBV S and GST-SASRS S samples using an anti-ε-COP antibody when the cell lysates had been prepared at pH 6.5. COPI coatomer components were also detected in purified SARS-CoV particles by Neuman et al. (2008). As the COPI coatomer is involved in the retrograde vesicular transport between Golgi and ER and in transport from the intermediate compartment to the *cis*-Golgi (Kirchhausen, 2000; Volpicelli-Daley et al., 2005) it may have a role in SARS-CoV and IBV assembly by concentrating the S protein at the site of coronavirus budding.

The GST pull-down assay is a long-known affordable approach to look for cellular interaction partners. Moreover, it was successfully used to demonstrate the interaction of coronaviral proteins with cellular proteins (McBride et al., 2007; Zhang et al., 2014). We performed a GST pull-down assay to identify cellular proteins that may interact with the TGEV S protein. The S protein of TGEV contains a tyrosine-based retention signal in the C-terminal part of its cytoplasmic domain (Schwegmann-Wessels et al., 2004). Recently, we have shown that this retention signal leads to the subcellular localization of the TGEV S protein at the ER-Golgi intermediate compartment (ERGIC), the site where coronavirus assembly and budding occurs (Paul et al., 2014). We assume that this localization is determined by the interaction of one or more cellular proteins with the tyrosine-based sorting signal present in TGEV S and that this interaction may play a role in virus assembly.

5.1. Cloning of GST constructs

We cloned the portion of the TGEV S protein gene encoding for the last 26 amino acids of the cytoplasmic domain into the pGEX-5x-1 vector (Fig. 1A). In addition to the wildtype sequence of the TGEV S protein, we mutated the tyrosine at position −10 to an alanine. This mutation is expected to abolish the interaction with cellular proteins responsible for the tyrosine-based retention of the TGEV S protein at the ERGIC. Full-length S protein mutants with a tyrosine to alanine mutation at this position are transported to the cell surface and not retained at the ERGIC (Schwegmann-Wessels et al., 2004). These two GST constructs, GST_TGEVS_26aa and GST_TGEVS(Y/A)_26aa, as well as the GST control were transformed into *E. coli* BL21 cells. Expression of the GST fusion proteins was induced by adding 0.1 mM isopropyl-β-D-thiogalactoside (IPTG). After 4 h of induction, bacterial cells were harvested, lysed, and sonicated. The GST fusion proteins were purified using Protino® Glutathione Agarose 4B (Macherey-Nagel, Germany). The two cloned GST fusion proteins and the GST control protein were detected, after SDS-PAGE and Coomassie Blue staining, at a molecular mass of about 30 kDa (Fig. 1B). Due to the addition of 26 amino acids of the TGEV S protein C-terminus, the wt and mutant protein migrated a little bit slower than GST alone.

5.2. GST pull-down assay

To identify proteins which may bind to the 26 amino acid stretch of the TGEV S protein we incubated cell lysates of IPI2I cells, an ileal wild boar cell line – susceptible to infection by TGEV – with the purified GST fusion proteins. For this purpose, IPI2I cell lysates containing comparable protein amounts were pre-incubated with Glutathione-agarose (for 1.5 h, 4 °C) before they were transferred to fresh beads that were pre-incubated for 1.5 h, 4 °C with the respective GST fusion proteins. After an additional incubation of 1.5 h at 4 °C, the samples were centrifuged and heated in SDS sample buffer at 96 °C. The proteins were separated by SDS-PAGE and stained with Coomassie Blue. In the sample, containing the GST_TGEVS_26aa and the IPI2I cell lysate an additional faint band at around 300 kDa was visible (Fig. 2). From all lanes containing cell lysates in the height of this band, gel slices were subjected to mass spectrometry analysis. In addition to trypsin and glutathione-transferase which were both detected in the GST_TGEVS_26aa + IPI2I and in the GST_TGEVS(Y/A)_26aa + IPI2I lanes, filamin A was identified in the lane containing the TGEV S wildtype fusion protein (to be published) with an electrophoretic mobility corresponding to a molecular mass of about 300 kDa. This fits to the known molecular

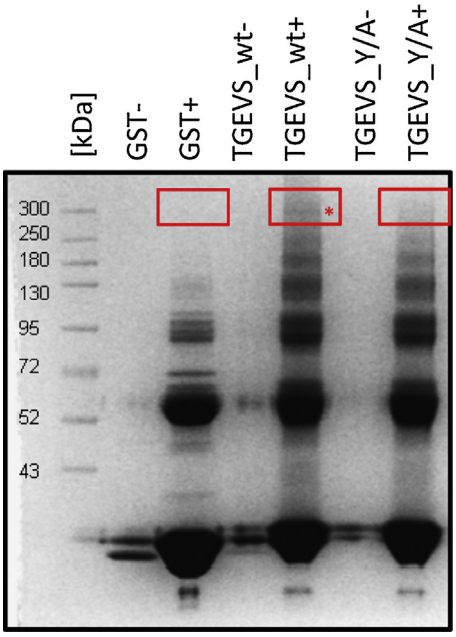

Fig. 2. Incubation of IPI2I cell lysates with the different GST fusion proteins (+). Gel slices on the height of the red boxes were excised from the gel and analyzed by mass spectrometry. The red star marks the detected band that may represent an interaction candidate of TGEVS_wt. As additional control, GST fusion proteins without cell lysates were loaded onto the gel (−).

mass of filamin A. It is not completely clear why filamin A was not detected in the lane with the TGEV S mutant fusion protein: maybe there was no interaction of both of them or the amount of proteins was too low for detection. As this identification was at least a hint for a potential interaction candidate, we focused on filamin A and its potential role in TGEV infection.

6. Filamin A: a cytostructural protein

Filamin A belongs to the actin-binding proteins (ABP). It crosslinks F-actin and forms orthogonal networks to bundles depending on their concentration (Popowicz et al., 2006; Tseng et al., 2004). Since the discovery of filamin A in 1975 over 90 binding partners like receptors, intracellular signaling molecules, transcription factors, and channels have been identified (Nakamura et al., 2011). In addition to F-actin, examples for filamin binding partners involved in cell adhesion, spreading, and migration are calmodulin, vimentin, ICAM-1, CEACAM1, Rho, and Rac (Del Valle-Perez et al., 2010; Jeon et al., 2008; Kanters et al., 2008; Kim et al., 2010; Klaile et al., 2005; Nakamura et al., 2005; Ohta et al., 1999). Filamin interacts with the cellular protease furin in sorting and stabilizing this protein (Liu et al., 1997). Due to the interaction of caveolin-1 and filamin the caveolae are anchored to the cytoskeleton (Stahlhut and van Deurs, 2000). Moreover, filamin A regulates the internalization of caveolae via its interaction with caveolin-1 and promotes caveolae clustering and trafficking (Sverdlov et al., 2009). Filamin A was also shown to play an important role in HIV infection. There, filamin A functions as an adaptor protein that links the HIV receptors to the actin cytoskeleton and causes clustering of the receptors (Jimenez-Baranda et al., 2007). Furthermore, filamin A interacts with the Gag protein and is involved in particle assembly of HIV 1 (Cooper et al., 2011).

6.1. Filamin A: a putative interaction candidate for the TGEV S protein

We started with the analysis of filamin A expression in the different cell lines we regularly use for experiments with the TGEV S protein: baby hamster kidney cells (BHK21), the aforementioned IPI2I cells, and swine testicular (ST) cells. Fig. 3B shows, that in these cell lines filamin A was detectable with an

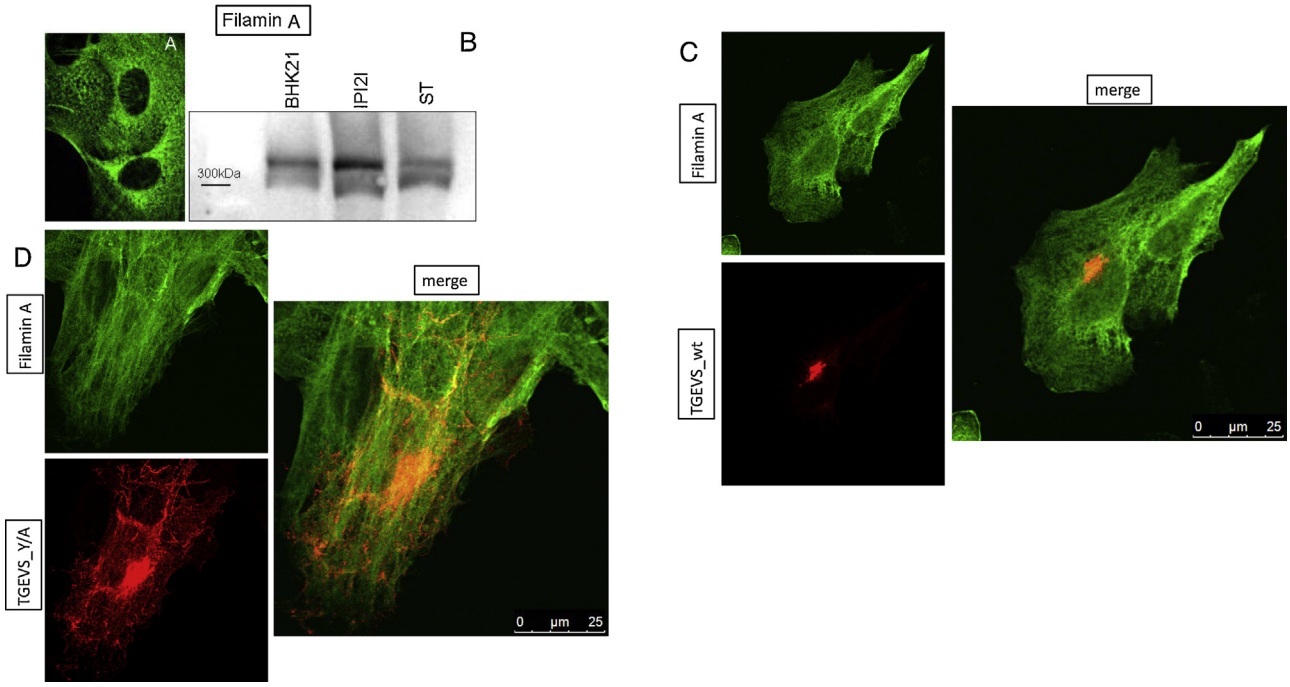

Fig. 3. Filamin A is present in different cell lines and co-localizes with the TGEV S protein. (A) Confocal microscopy of IPI2I cells stained with an anti-filamin A antibody and anti-rabbit Fitc. Filamin A is expressed all over the cytoplasm. (B) Detection of filamin A in BHK21, IPI2I, and ST cells at around 300 kDa in a Western blot analysis. (C/D) The full length cDNA encoding for the TGEVS wt protein (C) or for the TGEVS_Y/A mutant protein (D) was transfected into IPI2I cells. S protein was detected with a monoclonal anti-S antibody and an anti-mouse Rhodamin antibody (shown in red). Endogenous filamin A was detected with a monoclonal filamin A antibody and an anti-rabbit FITC antibody (shown in green). Co-localized proteins are visible in orange/yellow (merge).

anti-filamin A antibody from rabbit (Abcam) as a protein band at around 300 kDa (Fig. 3B). The confocal microscopy image of filamin A staining in IPI2I cells demonstrated that this cellular protein was distributed like a filamentous network all over the cytoplasm (Fig. 3A).

We transfected IPI2I cells with the full-length cDNA encoding for the TGEV S protein or the TGEV S Y/A mutant protein using lipofectamine™ 2000 (Life Technologies) and stained the S protein with a monoclonal anti-S antibody (6A.C3, kindly provided by Luis Enjuanes) and an anti-mouse Rhodamin antibody. The endogenic expression of filamin A was visualized by a monoclonal anti-filamin A antibody (Abcam) and an anti-rabbit FITC antibody. The co-localization of filamin A with the two different TGEV S proteins was analyzed by confocal microscopy (Fig. 3C and D). In those pictures, it seemed that there was a partial co-localization of both TGEV S proteins with filamin A. The TGEV S_Y/A protein was distributed all over the cell but in some cells a high amount of the mutant protein was concentrated at the ERGIC. We analyzed this by co-localization experiments with a GFP-ERGIC marker (data not shown).

6.2. Involvement of filamin A in TGEV infection

We wanted to find out if this putative interaction is detectable during a TGEV infection. Therefore, we infected ST cells with TGEV PUR 46 MAD and performed an immunofluorescence assay at different time points after infection. To find out whether the S protein of TGEV co-localizes with filamin A we analyzed the ST cells under the confocal microscope 2, 8, and 24 h after infection (Fig. 4). We found a partial co-localization of both proteins during infection, which appeared to be most obvious at 8 h post-infection. This may be a hint that filamin A is involved in TGEV assembly and incorporation of S protein into viral particles at the ERGIC. To verify this result, we immunoprecipitated ST cell lysates 8 h after infection with TGEV using an anti-S antibody. After Western blotting we were not able to detect filamin A in those immunoprecipitates although we obtained a strong filamin A band in ST cell lysates directly subjected to the Western blot analysis (data not shown). In our experiments the localization of filamin A was not obviously altered upon infection (Fig. 4). Further analyses have to be done to address this point.

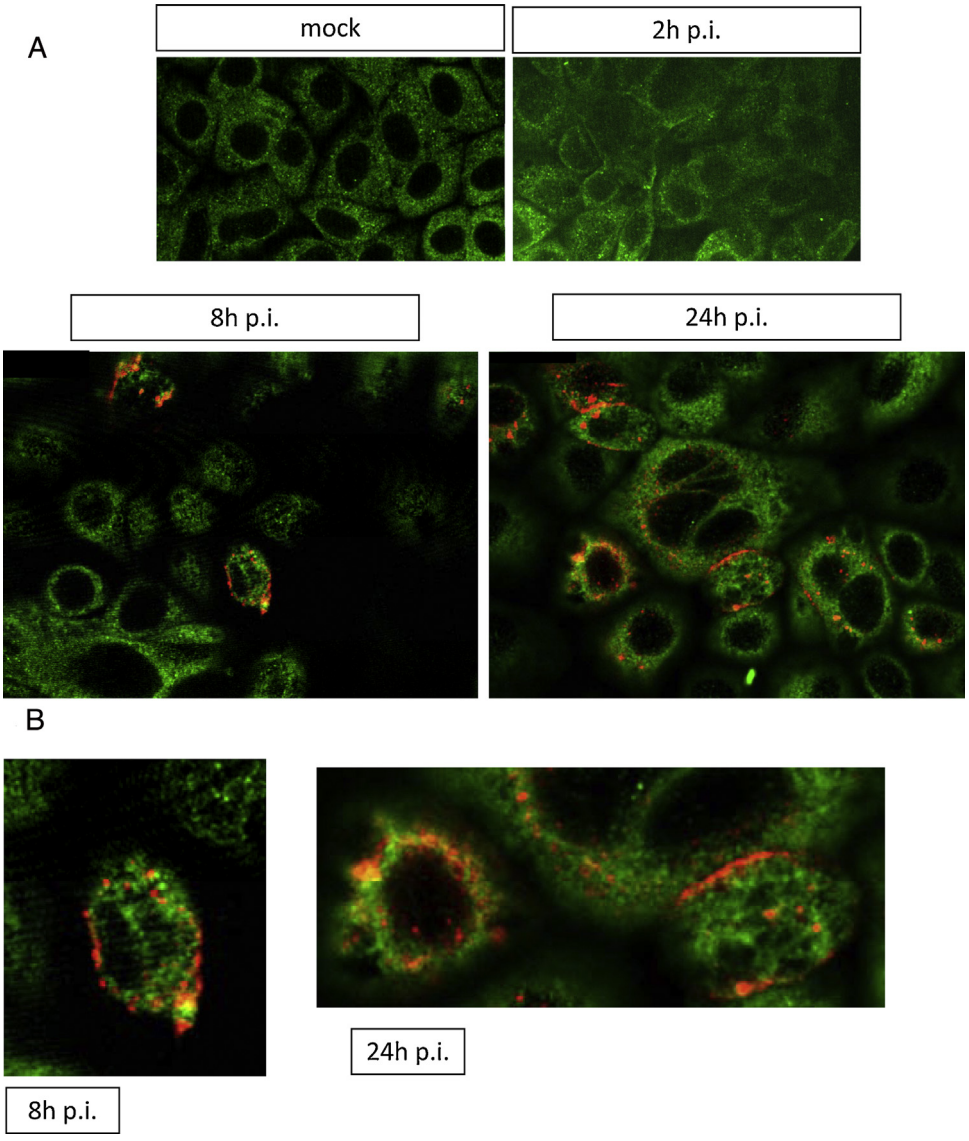

Fig. 4. Filamin A co-localizes with the S protein after TGEV infection. (A) ST cells were mock-infected or infected with TGEV PUR46 MAD. Immunofluorescence analysis using anti-filamin A antibody (green) and anti-TGEV S antibody (red) was performed 2, 8, and 24 h p.i. Pictures were taken with a Leica TCS SP5 confocal microscope. (B) Zoom of picture details at 8 and 24 h p.i.

Neuman and coworkers detected cytostructural proteins like actin, myosin, tubulin, fibronectin and also filamin in their proteinase K treated purified SARS-CoV preparations but also in "background samples" referred to as uninfected Vero-E6 cells (Neuman et al., 2008). They supposed that these cellular proteins are incorporated into the virions. According to this, we grew TGEV on ST cells, pelleted the virions from the cell culture supernatant after clarification, and purified the viral particles over a 20% to 50% sucrose gradient as described by Krempl and Herrler (2001). Samples with purified virions were separated by SDS-PAGE and stained with Coomassie Blue to visualize the respective viral proteins. In addition, one part of the purified TGE virions was separated by SDS-PAGE and compared with BHK21, IPI2I, and ST cell lysates for which we knew that they contain filamin A. In a Western blot analysis, we used the antibody against filamin A and detected this protein in the three cell lysates but not in our virus preparation (data not shown). Maybe filamin A is not present in TGEV particles or the amount of filamin A is too low to be detectable by Western Blot analysis. In mass spectrometry as performed by Neuman et al., we would probably be able to identify this low amount of filamin.

Which additional experiments can we perform to check the role of filamin A in TGEV infection? SiRNA experiments are an approach to verify the role of filamin A as interaction candidate for the TGEV S protein. After down-regulation of endogenous filamin A, changes in the transport of the TGEV S protein in transfected as well as in infected cells can be analyzed. A filamin A deficient melanoma cell line is known (Cunningham et al., 1992). A study of the TGEV S protein transport in such a cell line may also help to find out whether filamin A is important for the retention of the TGEV S protein at the ERGIC. Another approach would be the overexpression of filamin A in e.g. IPI2I cells to visualize the interaction of TGEV S with filamin A and to analyze its effect on TGEV replication.

In summary, filamin A may be an interaction candidate for the TGEV S protein. Due to its versatile role in cell structure and function, it is possible that it takes part in the assembly and budding process of coronaviruses. Further research – like the experiments described above – is necessary to validate and verify if and what role filamin A plays in the coronavirus life cycle.

Taken together, the different approaches summarized in this paper suggest that cellular proteins connected to the cytoskeleton are involved in the coronavirus replication cycle and are important for coronavirus assembly and budding.

Acknowledgments

Financial support was provided by a grant to C.S.-W. (SCHW1408/1.1) from the German Research Foundation (DFG). C.S.-W. is funded by the Emmy Noether program from the DFG.

The technical assistance of S. Bauer is highly appreciated.

We thank G. Herrler for critically reading the manuscript and A. Pich for mass spectrometry analysis. We thank L. Enjuanes for the monoclonal antibody 6A.C3 against the TGEV S protein. We thank R. Cattaneo for providing the pCG1 expression plasmid.

References

Aschenbrenner, L., Lee, T., Hasson, T., 2003. Myo6 facilitates the translocation of endocytic vesicles from cell peripheries. Mol. Biol. Cell 14, 2728–2743.

Backes, P., Quinkert, D., Reiss, S., Binder, M., Zayas, M., Rescher, U., Gerke, V., Bartenschlager, R., Lohmann, V., 2010. Role of annexin A2 in the production of infectious hepatitis C virus particles. J. Virol. 84, 5775–5789.

Beaton, A.R., Rodriguez, J., Reddy, Y.K., Roy, P., 2002. The membrane trafficking protein calpactin forms a complex with bluetongue virus protein NS3 and mediates virus release. Proc. Natl. Acad. Sci. U.S.A. 99, 13154–13159.

Bost, A.G., Prentice, E., Denison, M.R., 2001. Mouse hepatitis virus replicase protein complexes are translocated to sites of M protein accumulation in the ERGIC at late times of infection. Virology 285, 21–29.

Calvo, E., Escors, D., Lopez, J.A., Gonzalez, J.M., Alvarez, A., Arza, E., Enjuanes, L., 2005. Phosphorylation and subcellular localization of transmissible gastroenteritis virus nucleocapsid protein in infected cells. J. Gen. Virol. 86, 2255–2267.

Cantin, R., Methot, S., Tremblay, M.J., 2005. Plunder and stowaways: incorporation of cellular proteins by enveloped viruses. J. Virol. 79, 6577–6587.

Cao, Z., Han, Z., Shao, Y., Geng, H., Kong, X., Liu, S., 2011. Proteomic analysis of chicken embryonic trachea and kidney tissues after infection in ovo by avian infectious bronchitis coronavirus. Proteome Sci. 9, 11.

Cao, Z., Han, Z., Shao, Y., Liu, X., Sun, J., Yu, D., Kong, X., Liu, S., 2012. Proteomics analysis of differentially expressed proteins in chicken trachea and kidney after infection with the highly virulent and attenuated coronavirus infectious bronchitis virus in vivo. Proteome Sci. 10, 24.

Chertova, E., Chertov, O., Coren, L.V., Roser, J.D., Trubey, C.M., Bess Jr., J.W., Sowder 2nd, R.C., Barsov, E., Hood, B.L., Fisher, R.J., Nagashima, K., Conrads, T.P., Veenstra, T.D., Lifson, J.D., Ott, D.E., 2006. Proteomic and biochemical analysis of purified human immunodeficiency virus type 1 produced from infected monocyte-derived macrophages. J. Virol. 80, 9039–9052.

Cohen, J.R., Lin, L.D., Machamer, C.E., 2011. Identification of a Golgi complex-targeting signal in the cytoplasmic tail of the severe acute respiratory syndrome coronavirus envelope protein. J. Virol. 85, 5794–5803.

Cooper, J., Liu, L., Woodruff, E.A., Taylor, H.E., Goodwin, J.S., D'Aquila, R.T., Spearman, P., Hildreth, J.E., Dong, X., 2011. Filamin A protein interacts with human immunodeficiency virus type 1 Gag protein and contributes to productive particle assembly. J. Biol. Chem. 286, 28498–28510.

Corse, E., Machamer, C.E., 2000. Infectious bronchitis virus E protein is targeted to the Golgi complex and directs release of virus-like particles. J. Virol. 74, 4319–4326.

Corse, E., Machamer, C.E., 2002. The cytoplasmic tail of infectious bronchitis virus E protein directs Golgi targeting. J. Virol. 76, 1273–1284.

Corse, E., Machamer, C.E., 2003. The cytoplasmic tails of infectious bronchitis virus E and M proteins mediate their interaction. Virology 312, 25–34.

Cudmore, S., Reckmann, I., Way, M., 1997. Viral manipulations of the actin cytoskeleton. Trends Microbiol. 5, 142–148.

Cunningham, C.C., Gorlin, J.B., Kwiatkowski, D.J., Hartwig, J.H., Janmey, P.A., Byers, H.R., Stossel, T.P., 1992. Actin-binding protein requirement for cortical stability and efficient locomotion. Science 255, 325–327.

de Haan, C.A., Smeets, M., Vernooij, F., Vennema, H., Rottier, P.J., 1999. Mapping of the coronavirus membrane protein domains involved in interaction with the spike protein. J. Virol. 73, 7441–7452.

de Haan, C.A., Vennema, H., Rottier, P.J., 2000. Assembly of the coronavirus envelope: homotypic interactions between the M proteins. J. Virol. 74, 4967–4978.

Del Valle-Perez, B., Martinez, V.G., Lacasa-Salavert, C., Figueras, A., Shapiro, S.S., Takafuta, T., Casanovas, O., Capella, G., Ventura, F., Vinals, F., 2010. Filamin B plays a key role in vascular endothelial growth factor-induced endothelial cell motility through its interaction with Rac-1 and Vav-2. J. Biol. Chem. 285, 10748–10760.

Donnelly, S.R., Moss, S.E., 1997. Annexins in the secretory pathway. Cell. Mol. Life Sci. 53, 533–538.

Emmott, E., Munday, D., Bickerton, E., Britton, P., Rodgers, M.A., Whitehouse, A., Zhou, E.M., Hiscox, J.A., 2013. The cellular interactome of the coronavirus infectious bronchitis virus nucleocapsid protein and functional implications for virus biology. J. Virol. 87, 9486–9500.

Emmott, E., Rodgers, M.A., Macdonald, A., McCrory, S., Ajuh, P., Hiscox, J.A., 2010a. Quantitative proteomics using stable isotope labeling with amino acids in cell culture reveals changes in the cytoplasmic, nuclear, and nucleolar proteomes in Vero cells infected with the coronavirus infectious bronchitis virus. Mol. Cell Proteomics 9, 1920–1936.

Emmott, E., Smith, C., Emmett, S.R., Dove, B.K., Hiscox, J.A., 2010b. Elucidation of the avian nucleolar proteome by quantitative proteomics using SILAC and changes in cells infected with the coronavirus infectious bronchitis virus. Proteomics 10, 3558–3562.

Escors, D., Ortego, J., Laude, H., Enjuanes, L., 2001. The membrane M protein carboxy terminus binds to transmissible gastroenteritis coronavirus core and contributes to core stability. J. Virol. 75, 1312–1324.

Godeke, G.J., de Haan, C.A., Rossen, J.W., Vennema, H., Rottier, P.J., 2000. Assembly of spikes into coronavirus particles is mediated by the carboxy-terminal domain of the spike protein. J. Virol. 74, 1566–1571.

Gov, N.S., Gopinathan, A., 2006. Dynamics of membranes driven by actin polymerization. Biophys. J. 90, 454–469.

Greber, U.F., Way, M., 2006. A superhighway to virus infection. Cell 124, 741–754.

Harrist, A.V., Ryzhova, E.V., Harvey, T., Gonzalez-Scarano, F., 2009. Anx2 interacts with HIV-1 Gag at phosphatidylinositol (4,5) bisphosphate-containing lipid rafts and increases viral production in 293T cells. PLoS ONE 4, e5020.

Hay, J.C., Klumperman, J., Oorschot, V., Steegmaier, M., Kuo, C.S., Scheller, R.H., 1998. Localization, dynamics, and protein interactions reveal distinct roles for ER and Golgi SNAREs. J. Cell Biol. 141, 1489–1502.

He, R., Leeson, A., Ballantine, M., Andonov, A., Baker, L., Dobie, F., Li, Y., Bastien, N., Feldmann, H., Strocher, U., Theriault, S., Cutts, T., Cao, J., Booth, T.F., Plummer, F.A., Tyler, S., Li, X., 2004. Characterization of protein–protein interactions between the nucleocapsid protein and membrane protein of the SARS coronavirus. Virus Res. 105, 121–125.

Hiscox, J.A., Wurm, T., Wilson, L., Britton, P., Cavanagh, D., Brooks, G., 2001. The coronavirus infectious bronchitis virus nucleoprotein localizes to the nucleolus. J. Virol. 75, 506–512.

Jeon, Y.J., Choi, J.S., Lee, J.Y., Yu, K.R., Ka, S.H., Cho, Y., Choi, E.J., Baek, S.H., Seol, J.H., Park, D., Bang, O.S., Chung, C.H., 2008. Filamin B serves as a molecular scaffold for type I interferon-induced c-Jun NH2-terminal kinase signaling pathway. Mol. Biol. Cell 19, 5116–5130.

Jiang, X.S., Tang, L.Y., Dai, J., Zhou, H., Li, S.J., Xia, Q.C., Wu, J.R., Zeng, R., 2005. Quantitative analysis of severe acute respiratory syndrome (SARS)-associated coronavirus-infected cells using proteomic approaches: implications for cellular responses to virus infection. Mol. Cell. Proteomics 4, 902–913.

Jimenez-Baranda, S., Gomez-Mouton, C., Rojas, A., Martinez-Prats, L., Mira, E., Ana Lacalle, R., Valencia, A., Dimitrov, D.S., Viola, A., Delgado, R., Martinez, A.C., Manes, S., 2007. Filamin-A regulates actin-dependent clustering of HIV receptors. Nat. Cell Biol. 9, 838–846.

Kaelin Jr., W.G., Pallas, D.C., DeCaprio, J.A., Kaye, F.J., Livingston, D.M., 1991. Identification of cellular proteins that can interact specifically with the T/E1A-binding region of the retinoblastoma gene product. Cell 64, 521–532.

Kanters, E., van Rijssel, J., Hensbergen, P.J., Hondius, D., Mul, F.P., Deelder, A.M., Sonnenberg, A., van Buul, J.D., Hordijk, P.L., 2008. Filamin B mediates ICAM-1-driven leukocyte transendothelial migration. J. Biol. Chem. 283, 31830–31839.

Kim, H., Nakamura, F., Lee, W., Hong, C., Perez-Sala, D., McCulloch, C.A., 2010. Regulation of cell adhesion to collagen via beta1 integrins is dependent on interactions of filamin A with vimentin and protein kinase C epsilon. Exp. Cell Res. 316, 1829–1844.

Kirchhausen, T., 2000. Three ways to make a vesicle. Nat. Rev. Mol. Cell Biol. 1, 187–198.

Klaile, E., Muller, M.M., Kannicht, C., Singer, B.B., Lucka, L., 2005. CEACAM1 functionally interacts with filamin A and exerts a dual role in the regulation of cell migration. J. Cell Sci. 118, 5513–5524.

Klumperman, J., Locker, J.K., Meijer, A., Horzinek, M.C., Geuze, H.J., Rottier, P.J., 1994. Coronavirus M proteins accumulate in the Golgi complex beyond the site of virion budding. J. Virol. 68, 6523–6534.

Kong, Q., Xue, C., Ren, X., Zhang, C., Li, L., Shu, D., Bi, Y., Cao, Y., 2010. Proteomic analysis of purified coronavirus infectious bronchitis virus particles. Proteome Sci. 8, 29.

Krempl, C., Herrler, G., 2001. Sialic acid binding activity of transmissible gastroenteritis coronavirus affects sedimentation behavior of virions and solubilized glycoproteins. J. Virol. 75, 844–849.

Krijnse-Locker, J., Ericsson, M., Rottier, P.J., Griffiths, G., 1994. Characterization of the budding compartment of mouse hepatitis virus: evidence that transport from the RER to the Golgi complex requires only one vesicular transport step. J. Cell Biol. 124, 55–70.

Lim, K.P., Liu, D.X., 2001. The missing link in coronavirus assembly, retention of the avian coronavirus infectious bronchitis virus envelope protein in the pre-Golgi compartments and physical interaction between the envelope and membrane proteins. J. Biol. Chem. 276, 17515–17523.

Liu, G., Thomas, L., Warren, R.A., Enns, C.A., Cunningham, C.C., Hartwig, J.H., Thomas, G., 1997. Cytoskeletal protein ABP-280 directs the intracellular trafficking of furin and modulates proprotein processing in the endocytic pathway. J. Cell Biol. 139, 1719–1733.

Locker, J.K., Klumperman, J., Oorschot, V., Horzinek, M.C., Geuze, H.J., Rottier, P.J., 1994. The cytoplasmic tail of mouse hepatitis virus M protein is essential but not sufficient for its retention in the Golgi complex. J. Biol. Chem. 269, 28263–28269.

Machamer, C.E., Mentone, S.A., Rose, J.K., Farquhar, M.G., 1990. The E1 glycoprotein of an avian coronavirus is targeted to the cis Golgi complex. Proc. Natl. Acad. Sci. U.S.A. 87, 6944–6948.

McBride, C.E., Li, J., Machamer, C.E., 2007. The cytoplasmic tail of the severe acute respiratory syndrome coronavirus spike protein contains a novel endoplasmic reticulum retrieval signal that binds COPI and promotes interaction with membrane protein. J. Virol. 81, 2418–2428.

McBride, C.E., Machamer, C.E., 2010. A single tyrosine in the severe acute respiratory syndrome coronavirus membrane protein cytoplasmic tail is important for efficient interaction with spike protein. J. Virol. 84, 1891–1901.

Moss, S.E., Morgan, R.O., 2004. The annexins. Genome Biol. 5, 219.

Nakamura, F., Hartwig, J.H., Stossel, T.P., Szymanski, P.T., 2005. Ca^{2+} and calmodulin regulate the binding of filamin A to actin filaments. J. Biol. Chem. 280, 32426–32433.

Nakamura, F., Stossel, T.P., Hartwig, J.H., 2011. The filamins: organizers of cell structure and function. Cell. Adhes. Migr. 5, 160–169.

Neuman, B.W., Joseph, J.S., Saikatendu, K.S., Serrano, P., Chatterjee, A., Johnson, M.A., Liao, L., Klaus, J.P., Yates 3rd, J.R., Wuthrich, K., Stevens, R.C., Buchmeier, M.J., Kuhn, P., 2008. Proteomics analysis unravels the functional repertoire of coronavirus nonstructural protein 3. J. Virol. 82, 5279–5294.

Nguyen, V.P., Hogue, B.G., 1997. Protein interactions during coronavirus assembly. J. Virol. 71, 9278–9284.

Nogales, A., Marquez-Jurado, S., Galan, C., Enjuanes, L., Almazan, F., 2012. Transmissible gastroenteritis coronavirus RNA-dependent RNA polymerase and nonstructural proteins 2, 3, and 8 are incorporated into viral particles. J. Virol. 86, 1261–1266.

Ohta, Y., Suzuki, N., Nakamura, S., Hartwig, J.H., Stossel, T.P., 1999. The small GTPase RalA targets filamin to induce filopodia. Proc. Natl. Acad. Sci. U.S.A. 96, 2122–2128.

Orlinick, J.R., Chao, M.V., 1996. Interactions of cellular polypeptides with the cytoplasmic domain of the mouse Fas antigen. J. Biol. Chem. 271, 8627–8632.

Paul, A., Trincone, A., Siewert, S., Herrler, G., Schwegmann-Wessels, C., 2014. A lysine-methionine exchange in a coronavirus surface protein transforms a retention motif into an endocytosis signal. Biol. Chem. 395, 657–665.

Pfefferle, S., Schopf, J., Kogl, M., Friedel, C.C., Muller, M.A., Carbajo-Lozoya, J., Stellberger, T., von Dall'Armi, E., Herzog, P., Kallies, S., Niemeyer, D., Ditt, V., Kuri, T., Zust, R., Pumpor, K., Hilgenfeld, R., Schwarz, F., Zimmer, R., Steffen, I., Weber, F., Thiel, V., Herrler, G., Thiel, H.J., Schwegmann-Wessels, C., Pohlmann, S., Haas, J., Drosten, C., von Brunn, A., 2011. The SARS-coronavirus-host interactome: identification of cyclophilins as target for pan-coronavirus inhibitors. PLoS Pathog. 7, e1002331.

Ploubidou, A., Way, M., 2001. Viral transport and the cytoskeleton. Curr. Opin. Cell Biol. 13, 97–105.

Popowicz, G.M., Schleicher, M., Noegel, A.A., Holak, T.A., 2006. Filamins: promiscuous organizers of the cytoskeleton. Trends Biochem. Sci. 31, 411–419.

Radtke, K., Dohner, K., Sodeik, B., 2006. Viral interactions with the cytoskeleton: a hitchhiker's guide to the cell. Cell. Microbiol. 8, 387–400.

Rowland, R.R., Chauhan, V., Fang, Y., Pekosz, A., Kerrigan, M., Burton, M.D., 2005. Intracellular localization of the severe acute respiratory syndrome coronavirus nucleocapsid protein: absence of nucleolar accumulation during infection and after expression as a recombinant protein in vero cells. J. Virol. 79, 11507–11512.

Ryzhova, E.V., Vos, R.M., Albright, A.V., Harrist, A.V., Harvey, T., Gonzalez-Scarano, F., 2006. Annexin 2: a novel human immunodeficiency virus type 1 Gag binding protein involved in replication in monocyte-derived macrophages. J. Virol. 80, 2694–2704.

Sambrook, J., Russell, D.W., 2006. Detection of protein–protein interactions using the GST fusion protein pulldown technique. CSH Protoc., 2006.

Schwegmann-Wessels, C., Al-Falah, M., Escors, D., Wang, Z., Zimmer, G., Deng, H., Enjuanes, L., Naim, H.Y., Herrler, G., 2004. A novel sorting signal for intracellular localization is present in the S protein of a porcine coronavirus but absent from severe acute respiratory syndrome-associated coronavirus. J. Biol. Chem. 279, 43661–43666.

Shaw, M.L., Stone, K.L., Colangelo, C.M., Gulcicek, E.E., Palese, P., 2008. Cellular proteins in influenza virus particles. PLoS Pathog. 4, e1000085.

Simmons, G., Reeves, J.D., Rennekamp, A.J., Amberg, S.M., Piefer, A.J., Bates, P., 2004. Characterization of severe acute respiratory syndrome-associated coronavirus (SARS-CoV) spike glycoprotein-mediated viral entry. Proc. Natl. Acad. Sci. U.S.A. 101, 4240–4245.

Smith, D.B., Johnson, K.S., 1988. Single-step purification of polypeptides expressed in *Escherichia coli* as fusions with glutathione S-transferase. Gene 67, 31–40.

Stahlhut, M., van Deurs, B., 2000. Identification of filamin as a novel ligand for caveolin-1: evidence for the organization of caveolin-1-associated membrane domains by the actin cytoskeleton. Mol. Biol. Cell 11, 325–337.

Sverdlov, M., Shinin, V., Place, A.T., Castellon, M., Minshall, R.D., 2009. Filamin A regulates caveolae internalization and trafficking in endothelial cells. Mol. Biol. Cell 20, 4531–4540.

Timani, K.A., Liao, Q., Ye, L., Zeng, Y., Liu, J., Zheng, Y., Yang, X., Lingbao, K., Gao, J., Zhu, Y., 2005. Nuclear/nucleolar localization properties of C-terminal nucleocapsid protein of SARS coronavirus. Virus Res. 114, 23–34.

Tooze, J., Tooze, S., Warren, G., 1984. Replication of coronavirus MHV-A59 in sac-cells: determination of the first site of budding of progeny virions. Eur. J. Cell Biol. 33, 281–293.

Tseng, Y., An, K.M., Esue, O., Wirtz, D., 2004. The bimodal role of filamin in controlling the architecture and mechanics of F-actin networks. J. Biol. Chem. 279, 1819–1826.

Vennema, H., Godeke, G.J., Rossen, J.W., Voorhout, W.F., Horzinek, M.C., Opstelten, D.J., Rottier, P.J., 1996. Nucleocapsid-independent assembly of coronavirus-like particles by co-expression of viral envelope protein genes. EMBO J. 15, 2020–2028.

Vogels, M.W., van Balkom, B.W., Kaloyanova, D.V., Batenburg, J.J., Heck, A.J., Helms, J.B., Rottier, P.J., de Haan, C.A., 2011. Identification of host factors involved in coronavirus replication by quantitative proteomics analysis. Proteomics 11, 64–80.

Volpicelli-Daley, L.A., Li, Y., Zhang, C.J., Kahn, R.A., 2005. Isoform-selective effects of the depletion of ADP-ribosylation factors 1–5 on membrane traffic. Mol. Biol. Cell 16, 4495–4508.

von Brunn, A., Teepe, C., Simpson, J.C., Pepperkok, R., Friedel, C.C., Zimmer, R., Roberts, R., Baric, R., Haas, J., 2007. Analysis of intraviral protein–protein interactions of the SARS coronavirus ORFeome. PLoS ONE 2, e459.

Wang, J., Fang, S., Xiao, H., Chen, B., Tam, J.P., Liu, D.X., 2009. Interaction of the coronavirus infectious bronchitis virus membrane protein with beta-actin and its implication in virion assembly and budding. PLoS ONE 4, e4908.

Winter, C., Schwegmann-Wessels, C., Neumann, U., Herrler, G., 2008. The spike protein of infectious bronchitis virus is retained intracellularly by a tyrosine motif. J. Virol. 82, 2765–2771.

Wurm, T., Chen, H., Hodgson, T., Britton, P., Brooks, G., Hiscox, J.A., 2001. Localization to the nucleolus is a common feature of coronavirus nucleoproteins, and the protein may disrupt host cell division. J. Virol. 75, 9345–9356.

You, J., Dove, B.K., Enjuanes, L., DeDiego, M.L., Alvarez, E., Howell, G., Heinen, P., Zambon, M., Hiscox, J.A., 2005. Subcellular localization of the severe acute respiratory syndrome coronavirus nucleocapsid protein. J. Gen. Virol. 86, 3303–3310.

Zhang, X., Shi, H., Chen, J., Shi, D., Li, C., Feng, L., 2014. EF1A interacting with nucleocapsid protein of transmissible gastroenteritis coronavirus and plays a role in virus replication. Vet. Microbiol. 172, 443–448.

Zhang, X., Shi, H.Y., Chen, J.F., Shi, D., Lang, H.W., Wang, Z.T., Feng, L., 2013. Identification of cellular proteome using two-dimensional difference gel electrophoresis in ST cells infected with transmissible gastroenteritis coronavirus. Proteome Sci. 11, 31.

Zhou, B., Liu, J., Wang, Q., Liu, X., Li, X., Li, P., Ma, Q., Cao, C., 2008. The nucleocapsid protein of severe acute respiratory syndrome coronavirus inhibits cell cytokinesis and proliferation by interacting with translation elongation factor 1alpha. J. Virol. 82, 6962–6971.